Long-range interaction effects on calcium-wave propagation

W. D. Kepseu and P. Woafo*
Laboratory of Modeling and Simulation in Engineering and Biological Physics, Faculty of Science, University of Yaounde I, P.O. Box 812, Yaounde, Cameroon

(Received 16 November 2007; revised manuscript received 30 April 2008; published 29 July 2008)

In this paper, numerical simulation of calcium waves in a network of cells coupled together by a paracrine signaling is investigated. The model takes into account the long-range interaction between cells due to the action of extracellular messengers, which provide links between first-neighbor cells, but also on cells located far away from the excited cell. When considering bidirectional coupling, the long-range interaction influences neither the frequency nor the amplitude of oscillations, contrary to one-directional coupling. The long-range interaction influences the speed of propagation of Ca^{2+} waves in the network and induces enlargement of the transition zone before the steady regime of propagation is attained. We also investigate the long-range effects on the colonization of a given niche by a pathogenic microorganism signal on calcium wave propagation in the network.

DOI: 10.1103/PhysRevE.78.011922 PACS number(s): 87.18.Gh

I. INTRODUCTION

Calcium oscillations have been found in many animals [1,2] as well as in plant [3] cells, with many of these cells not having an obvious oscillatory biological function. The temporal behavior of cytoplasmic free calcium has attracted much attention, especially after it was shown that calcium concentrations display oscillatory behavior in response to agonist stimulation in a variety of cells [4,5]. Recently, it was observed in various systems that calcium signals can also mediate intercellular communication by eliciting or coordinating calcium signals in surrounding cells [6–10].

Physiological responses generated within a cell can propagate to neighboring cells through intercellular communication involving the passage of a molecular signal to a bordering cell through a gap junction [7–14], through extracellular communication, involving the secretion of molecular signals [14–18,20,21] (hormones, neurotransmitters, etc.), and more recently through extracellular calcium signaling [22–24]. However, the difference between these mechanisms is small as they all rely on the IP_3R (inositol-1,4,5-triphosphate receptors). The particular mechanism utilized depends primarily on the manner of stimulation and the extent of gap junction coupling (i.e., the cell types).

Evidence of the participation of an extracellular messenger as the source of Ca^{2+} intercellular wave propagation was demonstrated for the first time by Osipchuk and Cahalan [14] on gap junction intercellular deficient rat basophilic leukemia cells, with complete inhibition of the intercellular Ca^{2+} waves by suramin, a P_2-purinergic receptor inhibitor. They showed that cell stimulation induces the release of ATP (adenosine 5′-triphosphate), a Ca^{2+} agonist, from secretory granules, resulting in sufficiently large local increases in ATP concentration to trigger secondary calcium transients in neighboring contacting as well as noncontacting cells. Many other works have been done supporting the hypothesis that coordinated Ca^{2+} waves may occur through the activation of receptors by an extracellular messenger and that not all candidate messengers released by a cell can effectively communicate calcium signals [15,16,20], the exact type of messenger depending on the cell type. Most of these works focus on the action of extracellular messengers not only on neighboring cells directly in contact, but also on non contacting cells [14–16,19,20], indicating the long-range interaction in the network.

In recent years, experimental studies on Ca^{2+} waves have been carried out on different cells types, such as tracheal epithelial cells [25] and endothelial cells. Sneyd *et al.* [26,27] proposed a model for these intercellular waves, which assumes gap junction diffusion of inositol-1,4,5-triphosphate (IP_3) between adjacent cells. Mechanical stimulation of a single cell produces IP_3 within the cell, which in turn causes the release of Ca^{2+} from internal stores in the form of an intracellular Ca^{2+} wave. Diffusion of IP_3 between cells then initiates calcium waves in adjacent cells. This process continues as long as the amount of IP_3 entering a given cell is sufficient to induce a Ca^{2+} wave. Some recent papers following Sneyd *et al.* [26,27] have also studied the mechanisms that control the coordination and the intercellular propagation of calcium waves induced in other cell types, investigating the propagation of such intercellular Ca^{2+} waves in doublet and triplet cells [7,9,10,13,28,29]. They show that the gap junction coupling consists of a mechanism used by cells to coordinate and synchronize their information.

A fascinating aspect of bacterial models is the integration of bacterial-induced Ca^{2+} response in the strategy of diversion of host cell responses that is required for the establishment of the infectious disease. Pathways utilized by bacterial pathogens implicate timely and spatially controlled Ca^{2+} signaling within host cells. Bacterial pathogens can induce the cell release of ATP, which may expand bacterial cell signaling by a paracrine or autocrine route, leading to enhanced colonization or enhanced host cell responses to the invading microorganism [30,31]. Ca^{2+} responses induced by bacteria and bacterial products have been studied using *in vitro* cultured epithelial or phagocytic cells to get mechanistical in-

*Author to whom all correspondence should be addressed: pwoafo1@yahoo.fr

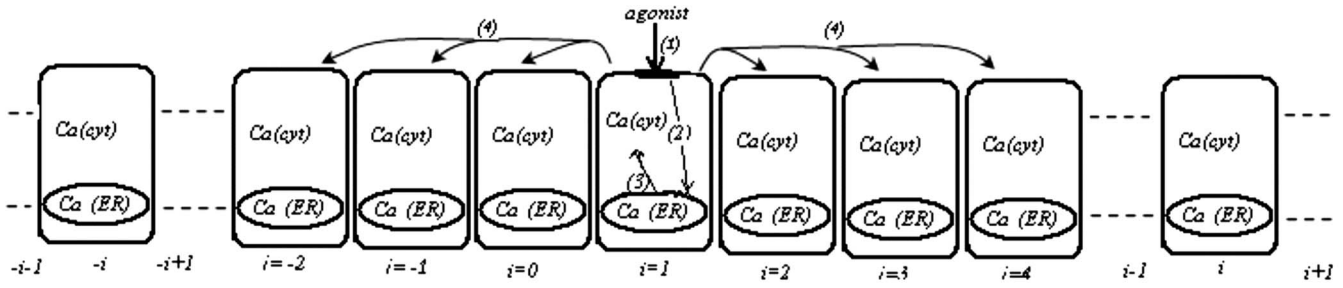

FIG. 1. Linear array of cells. Solid arrows depict reactions or transport steps. (1) Agonist link to the extracellular side of a receptor bound to a membrane, (2) second messenger (IP_3) bound to specific receptors in the membrane of an internal store of Ca^{2+} (endoplasmic reticulum), (3) large flux of calcium ions from the internal store into the cytosol, (4) long-range coupling.

sights into the mounting of the responses, as well as to establish links between Ca^{2+} signaling and bacterial induction of cellular processes relevant for the infectious pathology [32–34].

Following Ref. [35], in which the propagation of calcium waves in a network of cells coupled by paracrine signal has been elaborated on, thus putting into evidence the presence of two important zones of propagation in the network, it would be interesting now to see what are the effects that the long-range coupling has on the wave propagation, and also to know how in the virulence state of bacteria, long-range interaction influences the infection process. This constitutes the aim of this work. In Sec. II, we introduce the long-range interaction in a mathematical model and investigate by a numerical simulation its effects on Ca^{2+} oscillations and Ca^{2+} wave propagation. In Sec. III, we add infected cells in the network and investigate the effects of the long-range interaction on the colonization of a given niche by the infection. We also investigate how a calcium signal propagates when considering a one-direction flow of an extracellular messenger.

II. EFFECTS OF LONG-RANGE COUPLING ON Ca^{2+} PROPAGATION

To describe intercellular calcium oscillations in a network of cells, two aspects must be considered, namely the intracellular dynamics of calcium and the coupling between cells. Many models have been developed to explain Ca^{2+} oscillations in a cell [7,9–12,36,37]. Here, we choose the minimal model developed by Goldbetter *et al.* [36], for which we consider first that calcium extruded in one cell can stimulate its neighbors, and secondly, following Gracheva and Gunton [24], that cells are coupled together by assuming that the stimulus of the target cell is proportional to the cytosolic calcium content of its neighboring cells. The model described here is shown in Fig. 1. This one-dimensional chain up can be observed in protozoa that can live in an isolated state, but can also agglomerate if necessary. For example, the acrasial amoeba can form a multicellular structure when life conditions become unfavorable. This multicellular structure organizes itself on a longer rod on which spherical cells are fixed. The aggregation process is due to a substance that has been recognized as acrasine or AMPc. In certain approximations, our model could also explain how calcium propagates in multicellular structure such as epithelial cells, hepatocyte cells, liver cells, astrocytes, and others. Due to the fact that the extracellular messenger can be propagated via extracellular fluid to neighboring contacting cells as well as neighboring noncontacting cells [19,20], to model the long-range coupling between cells as shown in Fig. 1, we consider that the interaction coupling between cells i and j is

$$k_{ij} = k_0 \frac{1-r}{r} r^{|i-j|}, \tag{1}$$

where k_0 is the coupling coefficient between the first-neighbor cells and $r \in [0;1[$ is a parameter measuring the range of interaction. This type of interaction is well known in the context of condensed-matter physics [38]. The long-range interaction represents the influence of all cells at the neighborhood of a cell on its cytosolic Ca^{2+} oscillations. It can be seen as shown in Fig. 2(a) that the long-range coupling between cells increases when r increases. The variation of r can be related to that of the temperature or of the fluidity of the milieu. So, the number of cells interacting with a given cell depends on the fluidity and the temperature of the milieu. The absolute value $|i-j|$ represents the measure of the distance between cells of sites i and j. Figure 2(b) shows that the coupling between cells decreases gradually as the distance $|i-j|$ increases, this characterizing the fact that as the agonists propagate in the milieu, the number of receptors in the affected cells decreases.

As noted here before, to model intercellular calcium waves, two aspects must be considered: intracellular dynamics of calcium and coupling between cells. Two types of theoretical models have been developed so far: the spatiotemporal models and the temporal models. The spatiotemporal models take into account the fact that intracellular calcium waves are spatially distributed in cells. However, in some cell types with small diameter, such as hepatocytes (10–20 μm) [39,40] and pancreatic acinar cells (10–20 μm) [41], in which the intracellular propagation speed is of the order of 10 μm s^{-1} while intercellular propagation speed is around 120 μm s^{-1} [41], the spatial intracellular aspect can be neglected. Thus, the dynamics of the cells can be approximated by a set of ordinary differential equations. An interesting study by Tsaneva-Atanasova *et al.* [41] investigated in pancreatic acinar cells the temporal and the spatiotemporal models. Although the point-oscillator model (described by ordinary differential equations) cannot explain

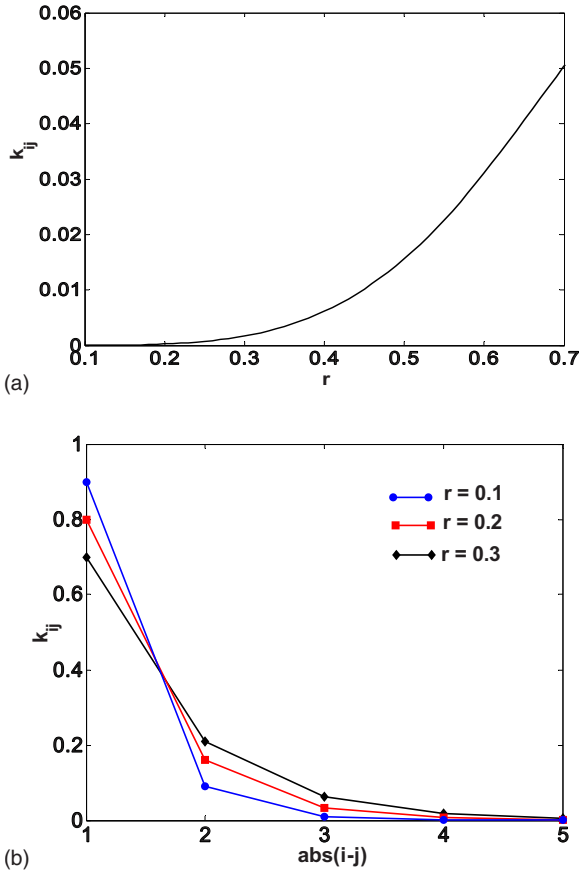

FIG. 2. (Color online) Coupling parameter behavior with $k_0=0.5$. (a) Under variation of the long-range parameter, $|i-j|=2$. (b) Under variation of the distance between the ith and the jth cells.

all the phenomena exhibited in the cell networks such as synchrony, it has been found in Ref. [41] that it gives a reasonably accurate general picture. That is why we use the temporal model in this paper.

For the mathematical modeling, let us consider x_i as the calcium concentration in the cytosol of the ith cell and y_i its internal store calcium concentration. Therefore, the calcium dynamics of the ith cell is described by the following set of equations:

$$\frac{dx_i}{dt} = a_i + k_0\frac{(1-r)}{r}\sum_{j\neq i}^{m} r^{|i-j|}(x_j - x_i) - V_{2,i} + V_{3,i} + k_f y_i - kx_i, \tag{2}$$

$$\frac{dy_i}{dt} = V_{2,i} - V_{3,i} - k_f y_i, \tag{3}$$

where $k_0=\beta V_1$, β represents the coupling parameter, $i=0$ to N, and $j=i-m$ to $i+m$, N being the total number of cells of the chain and m the order at which k_{ij} is negligible. Equations (2) and (3) were developed for the first time by Goldbetter *et al.* [36] to explain calcium oscillations in a cell and recently used to analyze intercellular calcium waves in a chain of diffusively coupled cells [35]. For this study, we have introduced the long-range interaction [see Eq. (1)]. In these equations,

$$a_i = \begin{cases} V_0 + bV_1 & \text{if } i = 1 \\ V_0 & \text{if } i \neq 1 \end{cases} \tag{4}$$

represents the term characterizing the excitation state of a cell. V_0 represents the influx of Ca^{2+} from the extracellular media and bV_1 represents a constant hormonal stimulus, which is localized on the first cell of the array (the one where the wave is initiated by the hormonal stimulus).

$$V_{2,i} = \frac{V_{m2}x_i^2}{k_2^2 + x_i^2}$$

represents the rate of Ca^{2+} pump from the cytosol to the internal store.

$$V_{3,i} = \frac{V_{m3}x_i^4 y_i^2}{(k_a^4 + x_i^4)(k_r^2 + y_i^2)}$$

represents the rate of Ca^{2+} liberation from the internal stores to the cytosol. The activation of this process is provoked by the Ca^{2+} itself, characterizing the calcium-induced calcium release (CICR) process. The Ca^{2+} extrusion from the cytosol to the extracellular media is taken into account by the term

TABLE I. Typical simulation constants for the minimal model.

Parameter	Value
k	2 s^{-1}
k_f	1.0 s^{-1}
k_2	1.0 μM
k_a	0.9 μM
k_r	2.0 μM
V_0	1.3 μM s^{-1}
V_1	7.3 μM s^{-1}
V_{m1}	65.0 μM s^{-1}
V_{m2}	500.0 μM s^{-1}
β	0.50

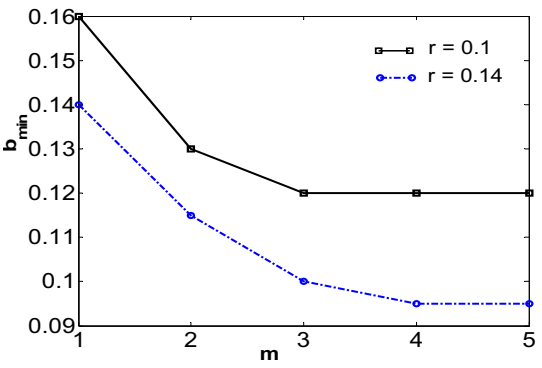

FIG. 3. (Color online) Variation of the minimal external hormonal stimulus required for calcium oscillations to occur and propagate in the chain when the range of interaction increases.

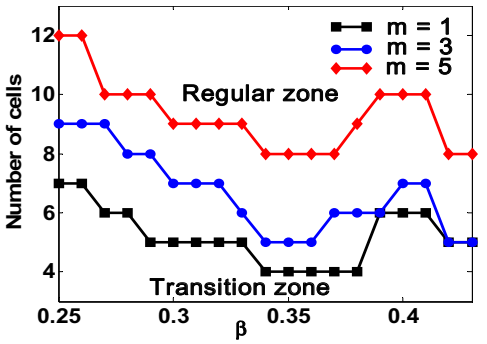

FIG. 4. (Color online) Boundary between the transition zone and the regular zone as one varies the hormonal stimulus with $r=0.1$.

kx_i. The Ca^{2+} can also pass from the internal stores to the cytosol via the passive flux given by the expression $k_f y_i$.

For the numerical simulation, we have considered an infinite chain of cells. This implies that a signal can be reproduced after N cells and thus the boundary conditions are taken to be cyclic and defined as

$$x_{i+N} = x_i,$$

$$y_{i+N} = y_i. \tag{5}$$

We integrate the set of equations (2) and (3) with relations (4) and (5) using the fourth-order Runge-Kutta algorithm [42], with a chain of $N=1000$ cells. The biological parameters of the equations are given in Table I. At rest, the concentrations of Ca^{2+} in the cytosol and in the internal store of each cell of the chain are taken to be $x_i(0)=0.2275$ μM and $y_i(0)=2.121\,96$ μM. It is found that the minimal agonist value required for the calcium wave to propagate decreases with the increase of the number of interacting cells as shown in Fig. 3. Therefore, for a given value of the long-range parameter r, one can determine the number of cells sensitive to extracellular messenger. Experimentally, the long-range length scale is not known; therefore, this work is a prediction for experimentalists to look for. Figure 3 also shows how the minimal agonist strength for calcium wave decreases with r.

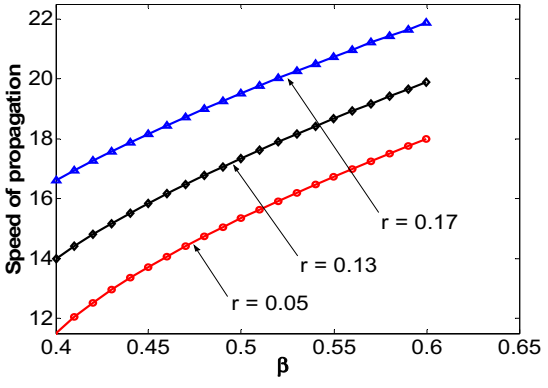

FIG. 5. (Color online) Speed of Ca^{2+} wave (number of cell s^{-1}) signal propagation in the chain when varying the coupling constant β with $m=5$.

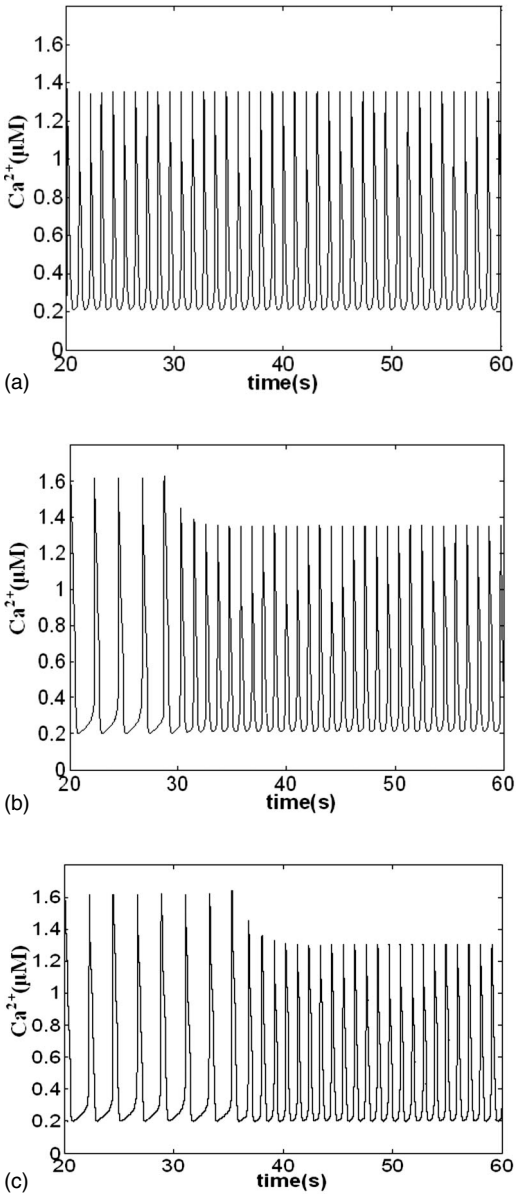

FIG. 6. Calcium oscillation of the bidirectional chain of cells at the neighborhood of the source of infection. (a) Behavior of the sick cell ($i=500$), $k=9$ s^{-1}. (b) Behavior of the cell $i=400$, $k=6$ s^{-1}. (c) Behavior of the cell $i=300$, $k=6$ s^{-1}.

This behavior is normal since the increase of the long-range parameter r implies the increase of the fluidity of the milieu.

A previous work studying the intercellular propagation of Ca^{2+} waves when considering only first-neighbor coupling showed that two zones of propagation are present [35]. In the first zone, called the transition zone, most of the phenomena observed in the study of a doublet or a triplet of cells are obtained. In the model with long-range interactions considered in this paper, we also find a similar complex dynamics in the transition zone as in the case of an array with only first-neighbor interactions between cells. This complex dynamics is characterized by Ca^{2+} oscillations displaying different maxima (main spike closely followed by smaller secondary ones), the number of spikes varying with the degree of excitation. The sequence finally yields oscillations that

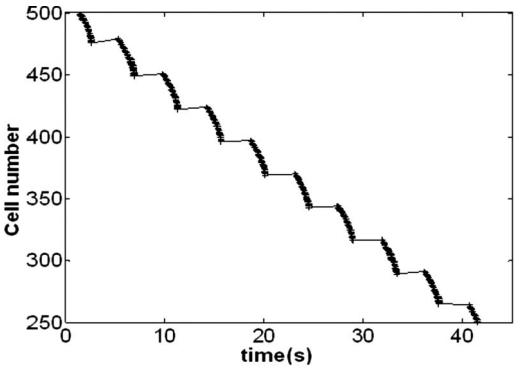

FIG. 7. Time at which cells in the network begin to exhibit illness behavior.

exhibit not only irregular numbers of simple spikes among complex double maxima, but also irregular spacing between the latter. This is the manifestation of chaos (see Ref. [35] for more details). The transition zone enlarges when the range of interaction increases (see Fig. 4). The second zone, called the regular or steady zone, is where the Ca^{2+} signal is identical from one cell to another (same amplitude and frequency of oscillations).

In a general manner, the long-range interaction parameter influences neither the frequency nor the amplitude of oscillations; it mainly induces the variation of the speed of propagation of the signal in the network. To determine the speed of a calcium signal propagating in the array, the following scheme is used. Let us assume that the maximal value of Ca^{2+} in the cytosol (generally more than 1 μM in our study) appears for the first time at a cell at time t_i, and that for cell j, the same maximal value appears also for the first time at t_j. Then the speed of the signal is the quantity $j-i$ divided by t_j-t_i. To determine t_i, the following procedure is used. For a cell i far from the excitation site, we note the quantities $Ca^{2+}(t-h)$, $Ca^{2+}(t)$, and $Ca^{2+}(t+h)$, h being the time step for the numerical simulation. The time t corresponds to t_i if $Ca^{2+}(t-h)<Ca^{2+}(t)$ and $Ca^{2+}(t)<Ca^{2+}(t+h)$. Figure 5 shows that the speed of Ca^{2+} oscillations in a network increases with the long-range parameter r and the coupling constant β. This is understandable, since it is known that Ca^{2+} oscillation birth in a cell depends on the number of calcium sensing receptors (CaRs) activated, and this birth extends further as the range of the interaction increases. Indeed, when the coupling parameter and the range of interaction increase, the number of CaRs affected in the adjacent cells increases.

III. EFFECT OF LONG-RANGE COUPLING ON LOCALIZED DISEASE

Ca^{2+} signals are implicated in various steps of bacterial infection. At the step of virulence, many enterotoxins have been found to induce an increase in the intracellular levels of Ca^{2+} in host cells [43–45]. By diffusing in the extracellular media, these toxins can act at a distance from the site of infection and have a global effect on the integrity of the epithelium by promoting the expression of proinflammatory

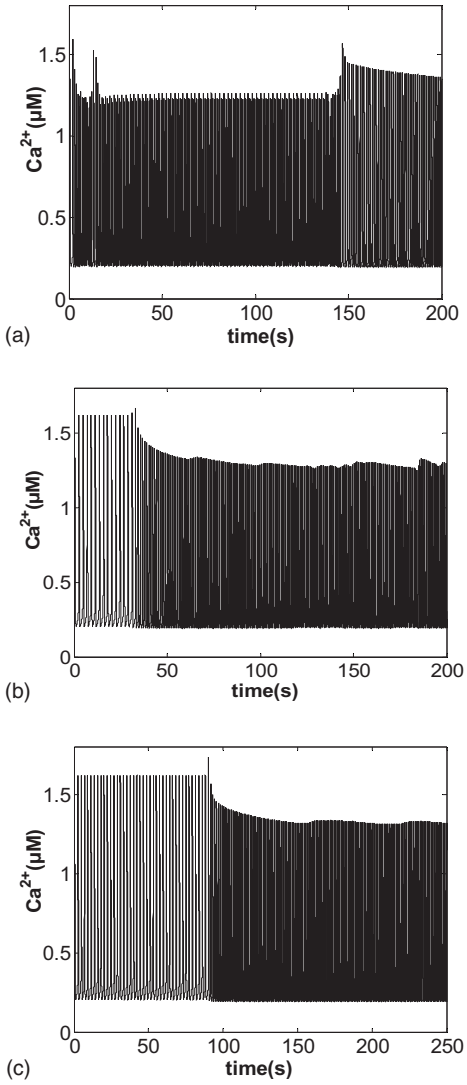

FIG. 8. Calcium oscillation of the one-directional chain of cells at the neighborhood of the source of infection. (a) Behavior of the sick cell (i=500). (b) Behavior of the cell (i=400). (c) Behavior of the cell (i=300).

cytokines leading to bacterial invasion and dissemination. Some bacterial toxins are cytotoxic because they induce the formation of large pores into host cell membranes. This transient pore-forming activity allows Ca^{2+} influx that leads to a long-lasting Ca^{2+} oscillating response. This Ca^{2+} influx appears independent of endogenous Ca^{2+} channels [46,47].

To characterize the Ca^{2+} influx in our study, we have considered as in Ref. [35] the term kx_i in the model, which represents the influx of Ca^{2+} from the cytosol to the extracellular space. We consider that when transient pores are formed in a cell, a large quantity of Ca^{2+} is extruded from the cytosol to the extracellular space independently of the calcium channels. Therefore, the coefficient k increases, characterizing the large spreading of bacteria toxins in the given niche.

We have considered for numerical investigations a chain of N=1000 cells in which we add ten infected cells at the center of the chain (i=490–500). Cells are considered healthy when k=6 s^{-1}, i.e., the extruded Ca^{2+} depends only

on calcium channels opening. For the sick cells, we take $k=9\ s^{-1}$. We can notice that, at the neighborhood of the source of infection, as the time increases, the chain exhibits oscillations similar to sick cells; this means that the neighboring cells perceive the effect of the liberated toxin (Fig. 6). Figure 7 shows the time at which cells of the network begin to exhibit illness behavior. One can see time intervals during which the abnormal behavior due to the disease remains localized in nearly one cell. Then the abnormal behavior propagates in the following cells progressively and quickly before another momentary stop in one cell. This quick propagation indicates that a set of cells exhibit illness behavior nearly at the same time. The number of cells in each set depends on the number m of interacting cells. In Fig. 7, where $m=12$, the set is made up of almost 24 cells because of the bidirectional coupling. The process of propagation of the illness continues as described above so that finally all the cells of the network exhibit the abnormal oscillations. We have found that the spreading speed increases with the long-range interaction parameter, meaning a rapid colonization of the network of cells by a pathogenic micro-organism as the range of interaction increases, e.g., by the increase of temperature and fluidity of the biological milieu. One can also note that the speed of propagation of the signal between the infected cells is greater than the speed of propagation of the signal between healthy cells.

Considering the fact that extracellular messengers can be transported by the fluid flow, it is reasonable to assume that only the cells that are in the flow direction will be affected. The one-directional propagation can be mathematically taken into consideration by setting $i=0$ to N and $j=i$ to $i+m$ in Eqs. (2) and (3). Considering the same condition as in Sec. III, one sees that the bacteria signals also colonize the array. However, the spread of calcium takes place in a manner not determined by the bacteria with not only a variation in frequencies, but also in amplitudes. As shown in Fig. 8, this amplitude variation is more pronounced at the neighborhood of infection source and becomes more regular as one moves away from the infection source. From the results of the numerical simulation, we have found that this irregularity of the amplitude variation does not disappear as the long-range interaction changes. This particular behavior of the calcium oscillations found here in a one-directional coupling model, around the colonization site, had been reported experimentally [43]. Finally, when we take into account the bidirectional coupling, we also find results indicating the increase of the speed of colonization of the cells in the network as the range of interaction increases.

IV. CONCLUSION

Here, we find out how the long-range interaction can affect the calcium wave propagation in a one-dimensional network of cells. The long-range interaction parameter can be related to the temperature or the fluidity of the biological milieu. It has been shown in this paper that the long-range interaction increases the speed of propagation of calcium waves and increases the length of the transition zone made up of cells exhibiting complex behaviors around the site of excitation. When some cells of the array are infected by a pathogenic micro-organism, e.g., a bacteria, the long-range interaction favors the propagation of the bacteria toxins or bacteria effects and thus induces a rapid colonization of the niche. The results also show that for the colonization of an array, the spread of calcium takes place with a variation of oscillation frequencies and irregularity in the amplitude variation.

For further studies, it will be interesting to include in our model the membrane plasma receptor dynamics similar to Riccobene *et al.* [48], and oscillations in IP_3 [49,50] as well as the spatiotemporal dynamics of each cells, thus having a network of coupled partial differential equations instead of a network of ordinary differential equations. It would also be interesting to investigate other models such as those based on a stochastic generalization of the fire-diffusive-fire Ca^{2+} release [51] and on a stochastic reaction diffusion array [52] in order to see whether the stochasticity can induce other complex phenomena. Moreover, a two-dimensional analysis of the model is of interest [53,54].

ACKNOWLEDGMENTS

P.W. acknowledges the support from the Alexander Von Humboldt Foundation and the Department of Nonlinear Dynamics at Max-Planck Institute for Dynamics and Self-organization, Gottingen (Germany).

[1] M. Rieutort, *Les Cellules dans l'Organisme, Physiologie Animale* (Masson, Paris, 1982).
[2] I. Schulz, E. Krause, A. González, A. Göbel, L. Sternfeld, and A. Schmid, Biol. Chem. **380**, 903 (1999).
[3] M. R. McAinsh, A. A. R. Webb, J. E. Taylor, and A. M. Hetherington, Plant Cell **7**, 1207 (1995).
[4] A. Goldbeter, *Biochemical Oscillations and Cellular Rhythms: The Molecular Basis of Periodic and Chaotic Behavior* (Cambridge University Press, Cambridge, 1996).
[5] E. C. Toescu, Am. J. Physiol. **269**, G173 (1995).
[6] L. Leybaert, K. Paemeleire, A. Strahonja, and M. J. Sanderson, Glia **24**, 398 (1998).
[7] T. Höfer, Biophys. J. **77**, 1244 (1999).
[8] S. Boitano, E. R. Dirksen, and M. J. Sanderson, Science **258**, 292 (1992).
[9] T. Höfer, A. Politi, and R. Heinrich, Biophys. J. **80**, 75 (2001).
[10] G. Dupont, Th. Tordjmann, C. Clair, St. Swillens, M. Claret, and L. Combettes, FASEB J. **14**, 279 (2000).
[11] J. Sneyd, J. Keizer, and M. J. Sanderson, FASEB J. **9**, 1463 (1995).
[12] M. Falcke, L. Tsimring, and H. Levine, Phys. Rev. E **62**, 2636 (2000).
[13] T. Höfer, L. Venance, and C. Giaume, J. Neurosci. **22**, 4850 (2002).

[14] B. E. Isakson, W. H. Evans, and S. Boitano, Am. J. Physiol. **280**, L221 (2001).
[15] Y. Osipchuk and M. Cahalan, Nature **359**, 241 (1992).
[16] M. K. Frame and A. W. De Feijter, Exp. Cell Res. **230**, 197 (1997).
[17] L. Homolya, T. H. Steinberg, and R. C. Boucher, J. Cell Biol. **150**, 1349 (2000).
[18] K. I. Enomoto, K. Furuya, S. Yamagishi, T. Oka, and T. Maeno, Pfluegers Arch. Eur. J. Physiol. **427**, 533 (1994).
[19] V. L. Cressman, E. Lazarowski, L. Homolya, R. C. Boucher, B. H. Koller, and B. R. Grubb, J. Biol. Chem. **274**, 26461 (1999).
[20] K. Enomoto, K. Furaya, S. Yamagashi, and T. Maeno, Cell Calcium **13**, 501 (1992).
[21] J. S. Marchant and I. Parker, J. Gen. Physiol. **116**, 691 (2000).
[22] A. M. Hofer, S. Curci, M. A. Doble, E. M. Brown, and D. I. Soybel, Nat. Cell Biol. **2**, 392 (2000).
[23] R. Caroppo, A. Gerbino, L. Debellis, O. Kifor, D. I. Soybel, E. M. Brown, A. M. Hofer, and S. Curci, EMBO J. **20**, 6316 (2001).
[24] M. E. Gracheva and J. D. Gunton, J. Theor. Biol. **221**, 513 (2003).
[25] M. Hansen, S. Boitano, E. R. Dirksen, and M. J. Sanderson, J. Cell. Sci. **106**, 995 (1993).
[26] J. Sneyd, B. Wetton, A. Charles, and M. J. Sanderson, Am. J. Physiol. **268**, C1 537 (1995).
[27] J. Sneyd, M. Wilkins, A. Stahonja, and M. Sanderson, Biophys. Chem. **72**, 101 (1998).
[28] Th. Tordjmann, B. Berthon, M. Claret, and L. Combettes, EMBO J. **16**, 5398 (1997).
[29] Th. Tordjmann, B. Berthon, E. Jacquemin, C. Clair, N. Stelly, G. Guillon, M. Claret, and L. Combettes, EMBO J. **17**, 4695 (1998).
[30] G. TranVan Nhieu, C. Clair, R. Bruzzone, M. Mesnil, P. Sansonetti, and L. Combettes, Nat. Cell Biol. **8**, 720 (2003).
[31] N. McNamara, A. Khong, D. McKemy, M. Caterina, J. Boyer, D. Julius, and C. Basbaum, Proc. Natl. Acad. Sci. U.S.A. **98**, 9086 (2001).
[32] E. J. Pettit and M. B. Hallett, J. Cell. Sci. **109**, 1689 (1996).
[33] E. J. Pettit and M. B. Hallett, J. Cell. Sci. **111**, 2209 (1998).
[34] S. Dewitt and M. B. Hallett, J. Cell Biol. **159**, 1 (2002).
[35] W. D. Kepseu and P. Woafo, Phys. Rev. E **73**, 041912 (2006).
[36] A. Goldbeter, G. Dupont, and M. J. Berridge, Proc. Natl. Acad. Sci. U.S.A. **87**, 1461 (1990).
[37] A. C. Ventura, L. Bruno, and S. P. Dawson, Phys. Rev. E **74**, 011917 (2006).
[38] P. Woafo, T. C. Kofane, and A. S. Bokosah, Phys. Rev. B **48**, 10153 (1993).
[39] G. Dupont, S. Swillens, C. Clair, T. Tordjmann, and L. Combettes, Biochim. Biophys. Acta **1498**, 134 (2000).
[40] G. Dupont, T. Tordjmann, C. Clair, S. Swillens, M. Claret, and L. Combettes, FASEB J. **14**, 279 (2000).
[41] K. Tsaneva-Atanasova, D. I. Yule, and J. Sneyd, Biophys. J. **88**, 1535 (2005).
[42] J. D. Lambert and D. S. Lambert, *Numerical Methods for Ordinary Differential Systems: The Initial Value Problem* (Wiley, New York, 1991).
[43] A. Ogawa, J. I. Katop, H. Watanabe, G. B. Nair, and T. Takeda, Infect. Immun. **58**, 3325 (1990).
[44] A. G. Chaudhuri and U. Ganguly, Biochim. Biophys. Acta **1267**, 131 (1995).
[45] A. G. Chaudhuri, J. Bhattacharya, G. B. Nair, T. Takeda, and M. K. Chakrabarti, FEMS Microbiol. Lett. **160**, 125 (1998).
[46] G. TranVan Nhieu, C. Clair, G. Grompone, and P. Sansonetti, Biol. Cell **96**, 93 (2004).
[47] H. Repp *et al.*, Cell. Microbiol. **4**, 483 (2002).
[48] T. A. Riccobene, G. M. Omann, and J. J. Linderman, J. Theor. Biol. **200**, 207 (1999).
[49] M. S. Nash, K. W. Young, R. A. Challis, and S. R. Nahorski, Nature **413**, 381 (2001).
[50] C. W. Taylor and P. Thorn, Curr. Biol. **11**, R352 (2001).
[51] S. Coombes and Y. Timofeeva, Phys. Rev. E **68**, 021915 (2003).
[52] N. Guisoni and M. J. de Oliveira, Phys. Rev. E **74**, 061905 (2006).
[53] M. E. Harris-White, S. A. Zanotti, S. A. Frautschy, and A. C. Charles, J. Neurophysiol. **79**, 1045 (1998).
[54] M. Wilkins and J. Snyed, J. Theor. Biol. **80**, 188 (1998).